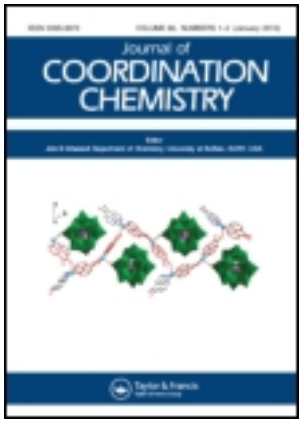

Journal of Coordination Chemistry
Publication details, including instructions for authors and subscription information:
http://www.tandfonline.com/loi/gcoo20

Structural, spectroscopic, and biological studies of N,O donor Schiff base copper(II) complexes

R.N. Patel [a], Anurag Singh [a], K.K. Shukla [a], Dinesh K. Patel [a] & V.P. Sondhiya [a]

[a] Department of Chemistry, A.P.S. University, Rewa 486003, Madhya Pradesh, India

Published online: 25 Feb 2011.

To cite this article: R.N. Patel, Anurag Singh, K.K. Shukla, Dinesh K. Patel & V.P. Sondhiya (2011) Structural, spectroscopic, and biological studies of N,O donor Schiff base copper(II) complexes, Journal of Coordination Chemistry, 64:5, 902-919, DOI: 10.1080/00958972.2011.558195

To link to this article: http://dx.doi.org/10.1080/00958972.2011.558195

Journal of Coordination Chemistry
Vol. 64, No. 5, 10 March 2011, 902–919

Taylor & Francis
Taylor & Francis Group

Structural, spectroscopic, and biological studies of N,O donor Schiff base copper(II) complexes

R.N. PATEL*, ANURAG SINGH, K.K. SHUKLA, DINESH K. PATEL and V.P. SONDHIYA

Department of Chemistry, A.P.S. University, Rewa 486003, Madhya Pradesh, India

(*Received 18 August 2010; in final form 13 December 2010*)

The Schiff bases (L^1 and L^2) and their complexes [$Cu(L)_2$] ($L^1 = N$-[(1)-1-(4-methylphenyl) ethylidene]benzolhydrazide and $L^2 = N$-[(1)-1-(2-methoxyphenyl)ethylidene]benzolhydrazide) have been prepared and characterized by elemental analysis, magnetic, and conductivity measurements. Crystal structure of the two complexes determined by single crystal X-ray analysis shows distorted square planar CuN_2O_2 coordination. Electron paramagnetic resonance spectra of these complexes in frozen DMSO show a signal at *g ca* 2. The trend in *g*-value ($g_\parallel > g_\perp > 2.0023$) suggests that the unpaired electron on copper(II) has $d_{x^2-y^2}$ character. The superoxide dismutase and biological (antimicrobial) activities of these complexes have also been screened.

Keywords: Copper(II) complexes; Biological activities; Superoxide dismutase activity; Electron paramagnetic resonance

1. Introduction

Copper is an essential element involved in several biological functions, a catalytic component of many metalloenzymes, including superoxide dismutase (SOD). A copper(II) complex which possesses SOD mimetic activity should have a flexible arrangement of ligands around copper(II) to allow easy reduction to Cu(I). In addition, a copper(II) SOD mimetic complex should have stability, avoiding dissociation in the acid region and should possess an accessible site in order to easily bind O_2^- radical and hence give quick reduction to Cu(I). Finally, an equatorial field of medium strength is required because strong fields do not favor attack of O_2^- to the apical sites [1–3].

Preclinical studies have revealed that SOD enzymes play a protective effect in several diseases. However, therapeutic use of the native SOD has several limitations related to low cell permeability and short half-life. Bovine CuZn-SOD was tested in clinical trials but immunological problems led to withdrawal from the market [4].

Supramolecular architectures through selective and directional non-covalent forces such as hydrogen bonding [5], π–π [6] and C–H $\cdots$ π [7] interactions in metallo-organic

*Corresponding author. Email: rnp64@ymail.com

ISSN 0095-8972 print/ISSN 1029-0389 online © 2011 Taylor & Francis
DOI: 10.1080/00958972.2011.558195

frameworks have potential applications as functional materials; 2,2′-bipyridine may form π–π and C–H$\cdots\pi$ interactions through pyridine planes, leading to different crystalline aggregates.

A number of Schiff bases and their metal complexes have been reported [8–13]. Here, we report the preparation and biological activity of Schiff bases and their transition metal complexes: [L^1] (**1**), [L^2] (**2**), [$Cu(L^1)_2$] (**3**), [$Cu(L^2)_2$] (**4**). Our aim is to modify the coordination environment of SOD mimics for better understanding of the SOD enzyme. The ability of these copper(II) complexes to scavenge O_2^- was evaluated by the nitro blue tetrazolium (NBT) method. Spectroscopic studies were performed in order to correlate the structural features of the complexes with their scavenging activity.

2. Experimental

2.1. *Materials*

Copper(II) nitrate trihydrate was purchased from S.d. fine-chemicals, India. All other chemicals used were of synthetic grade and used without purification.

2.2. *Physical measurements*

2.2.1. Magnetic measurements. Magnetic susceptibility measurements were made on a Gouy balance using a mercury(II) tetrathiocynato cobaltate(II) as calibrating agent ($\chi_g = 16.44\times10^{-6}$ c.g.s. units). The molar susceptibilities were corrected for diamagnetism of the constituent atoms by using Pascal constants.

2.2.2. Spectroscopy. UV-Vis spectra were recorded at 25°C on a Shimadzu UV-Vis recording spectrophotometer UV-1601 in quartz cells. IR-spectra were recorded in KBr on a Perkin-Elmer 783 spectrophotometer. X-band (~9.4 GHz) Electron paramagnetic resonance (EPR) spectra were recorded with a Varian E-line Century Series Spectrometer equipped with a dual cavity and operating at X-band with 100 kHz modulation frequency at room temperature and at 77 K. TCNE was used as field marker. Frozen solutions at 77 K used for EPR spectra were 3×10^{-3} mol L^{-1} in DMSO. The EPR parameters for copper(II) complexes were determined accurately using a simulation program [14].

2.2.3. Electrochemistry. Cyclic voltammetry was carried out with a BAS-100 Epsilon electrochemical analyzer having an electrochemical cell with a three-electrode system; Ag/AgCl was used as a reference electrode, glassy carbon as working electrode and platinum wire as an auxiliary electrode. 0.1 mol L^{-1} $NaClO_4$ was used as supporting electrolyte and DMSO as solvent. All measurements were carried out at 298 K under nitrogen.

2.2.4. Bioactivity. Antimicrobial (antibacterial) and SOD activities were evaluated using the following methods.

2.2.4.1. *SOD activity*. The *in vitro* SOD activity was measured using alkaline DMSO as a source of superoxide radical (O_2^-) and NBT as an O_2^- scavenger [15]. In general, 400 μL sample to be assayed was added to a solution containing 2.1 mL of 0.2 mol L^{-1} potassium phosphate buffer (pH 8.6) and 1 mL of 56 μmol L^{-1} alkaline DMSO solution while stirring. The absorbance was then monitored at 540 nm against a sample prepared under similar condition in non-alkaline DMSO.

2.2.4.2. *Antibacterial activity measurements*. The *in vitro* antimicrobial (antibacterial) activities of these complexes were tested using the paper disc diffusion method [16]. The chosen strain was *Escherichia coli*. The liquid containing the bacterial subcultures was autoclaved for 20 min at 121°C and at 15 lb pressure before inoculation. The bacteria were then cultured for 24 h at 36°C in an incubator. Nutrient agar was poured into a plate and allowed to solidify. The test compounds (DMSO solutions) were added dropwise to a 10 mm diameter filter paper disc placed at the center of each agar plate. The plates were kept at 5°C for 1 h, then transferred to an incubator maintained at 36°C. The width of the growth inhibition zone around the disc was measured after 24 h incubation.

2.3. *Synthesis*

2.3.1. Synthesis of L^1 (1). The Schiff base was prepared by condensation of 4-methylacetophenone and benzoylhydrazine. A solution of 4-methylacetophenone (10.0 mmol, 1.348 g) was added to solution of benzolhydrazine (10.0 mmol, 1.361 g) in ethanol (10 mL). The resulting solution was refluxed for 4 h after addition of 1–2 drops of acetic acid. On cooling the solution at room temperature, pale yellow crystals separated were filtered and washed with methanol. The product was recrystallized in high yield from hot ethanol and stored in a $CaCl_2$ desiccator, yield 0.23 g (92%). Anal. Calcd for $C_{16}H_{16}N_2O$ (**1**): C, 76.16; H, 6.39; N, 11.10%. Found: C, 76.06; H, 6.25; N, 11.02%.

2.3.2. Synthesis of L^2 (2). A solution of 2-methoxyacetophenone (10.0 mmol, 1.501 g) in 10 mL ethanol was refluxed with ethanolic solution of benzoylhydrazine (10.0 mmol, 1.361 g) continuously for 4 h after adding 1–2 drops of acetic acid. On cooling to room temperature, yellow crystals formed which were filtered and washed with methanol. The product was recrystallized in high yield from hot ethanol and stored in a $CaCl_2$ desiccator, yield 0.25 g (93%). Anal. Calcd for $C_{16}H_{16}N_2O_2$ (**2**): C, 71.62; H, 6.01; N, 10.44%. Found: C, 71.49; H, 5.95; N, 10.21%.

2.3.3. Synthesis of $[Cu(L^1)_2]$ (3). To a methanolic solution (20 mL) of cupric nitrate trihydrate (1.0 mmol, 0.241 g) a solution of L^1 (1.0 mmol, 0.252 g) in methanol was added with constant stirring at room temperature for 30 min. The solution was filtered and allowed to stand at room temperature for a few days. Blue crystals suitable for single crystal X-ray diffraction were recovered from the mother liquor and stored in a $CaCl_2$ desiccator, yield 0.47 g (83%). Anal Calcd for $C_{32}H_{30}CuN_4O_2$ (**3**): C, 67.82; H, 5.29; N, 9.89, Cu, 11.30%. Found: C, 67.75; H, 5.20; N, 9.76, Cu, 11.33%.

2.3.4. Synthesis of $[Cu(L^2)_2]$ (4). To a methanolic solution (20 mL) of copper(II) nitrate trihydrate (1.0 mmol, 0.241 g), a solution of L^2 (1.0 mmol, 0.316 g) in methanol was added and stirred for 1 h at room temperature. The solution was filtered and allowed to stand at room temperature for 1 day. Blue crystals suitable for single crystal X-ray diffraction were recovered from the mother liquor and stored in a $CaCl_2$ desiccator, yield 0.53 g (89%). Anal Calcd for $C_{32}H_{30}CuN_4O_4$ (**4**): C, 64.19; H, 5.01; N, 9.36, Cu, 10.69%. Found: C, 64.06; H, 4.95; N, 9.29, Cu, 10.75%.

2.3.5. Crystal structure determination. Single crystals for L^1, $[Cu(L^1)_2]$, and $[Cu(L^2)_2]$ were grown by slow evaporation of the reaction mixtures at room temperature. Single crystals suitable for X-ray analysis of **1**, **3** and **4** were mounted on a glass fiber and used for data collection. Crystal data were collected on an Enraf-Nonius $MACH_3$ diffractometer using graphite monochromated MoK_α radiation ($\lambda = 0.71073$ Å). The crystal orientation, cell refinement, and intensity measurements were made using CAD-4PC performing ψ-scan measurements. The structures were solved by direct methods using SHELXS-97 [17] and refined by full-matrix least-squares against F^2 using SHELXL-97 [18]. All non-hydrogen atoms were refined anisotropically. All hydrogens were geometrically fixed and allowed to refine using a riding model.

3. Results and discussion

3.1. *Synthesis*

In general, stoichiometric amounts of cupric nitrate trihydrate and ligand were taken separately and then the resulting solutions were mixed. The obtained products from the mixed solution were filtered off and dried. Both complexes were synthesized by the following sequential routes schemes 1 and 2.

3.2. *Crystal structure of L^1 (1)*

The ORTEP [19] view of **1** is shown in figure 1. Crystal structure refinement data related to **1** are given in table 1. The main bond angles and distances are presented in table 2. Complex **1** crystallized in the monoclinic crystal system, $P2_1/c$ space group and shows a Z configuration with respect to the C(8)–N(1) bond. The N(1)–N(2) = 1.388(3) and N(1)–C(8) = 1.279(13) Å are almost equal to those of **3** whereas the distance C(7)–O(1) = 1.226(3) is smaller than that of **3**, showing that this is a double bond. Delocalization is established in **3** between N(2)–C(1) and C(1)–O(1), with mononegative ligand. Therefore, the configuration of the ligand in the solid state is illustrated for its coordination with the metal as an NO donor, uninegative bidentate chelate. The N(1)–C(8) distance of 1.279 (3) Å close to theoretically predicted for a C=N double bond (1.28 Å) [20], confirming formation of Schiff-base [21].

A notable feature of the crystal structure of L^1 is formation of intramolecular H-bonding through the azo nitrogen, amide nitrogen (NH), and ketonic oxygen. The ligand forms hydrogen-bonded chains which run parallel to the crystallographic *c*-axis. We have observed the intramolecular hydrogen-bonding interaction

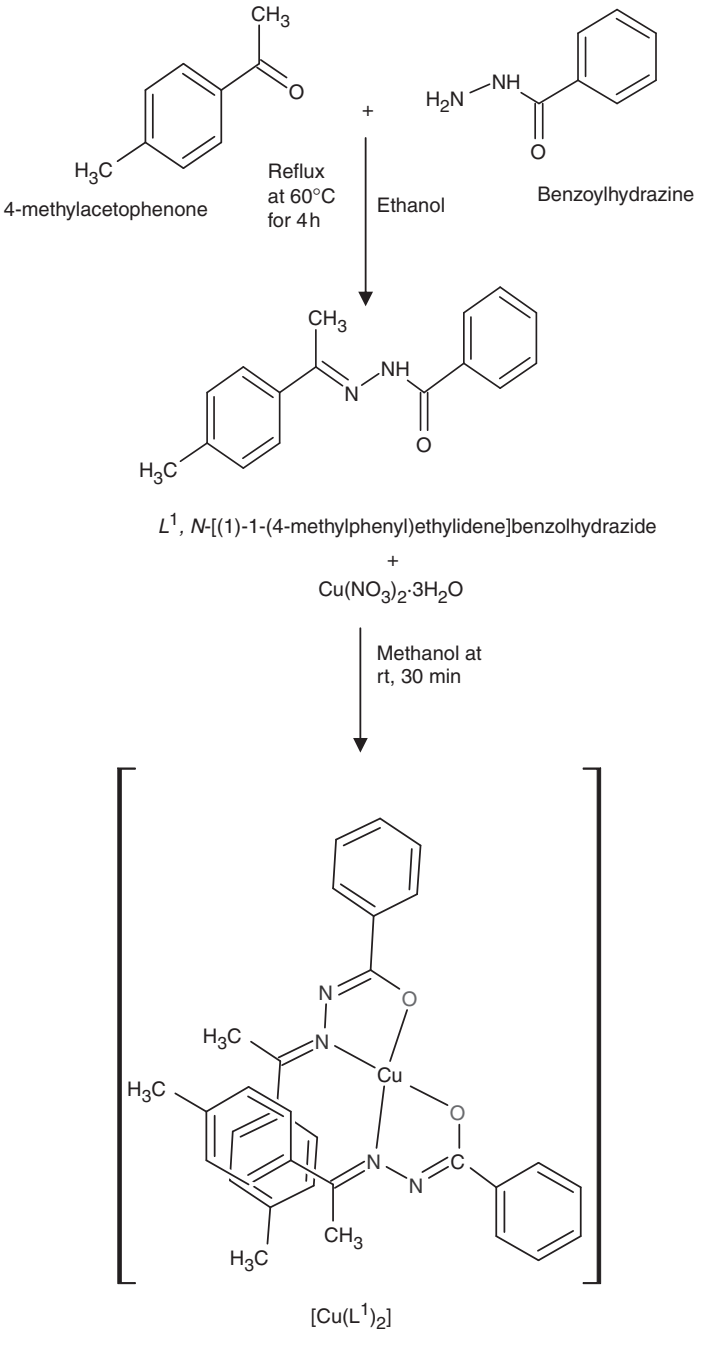

Scheme 1. Synthesis of L^1 and **3**.

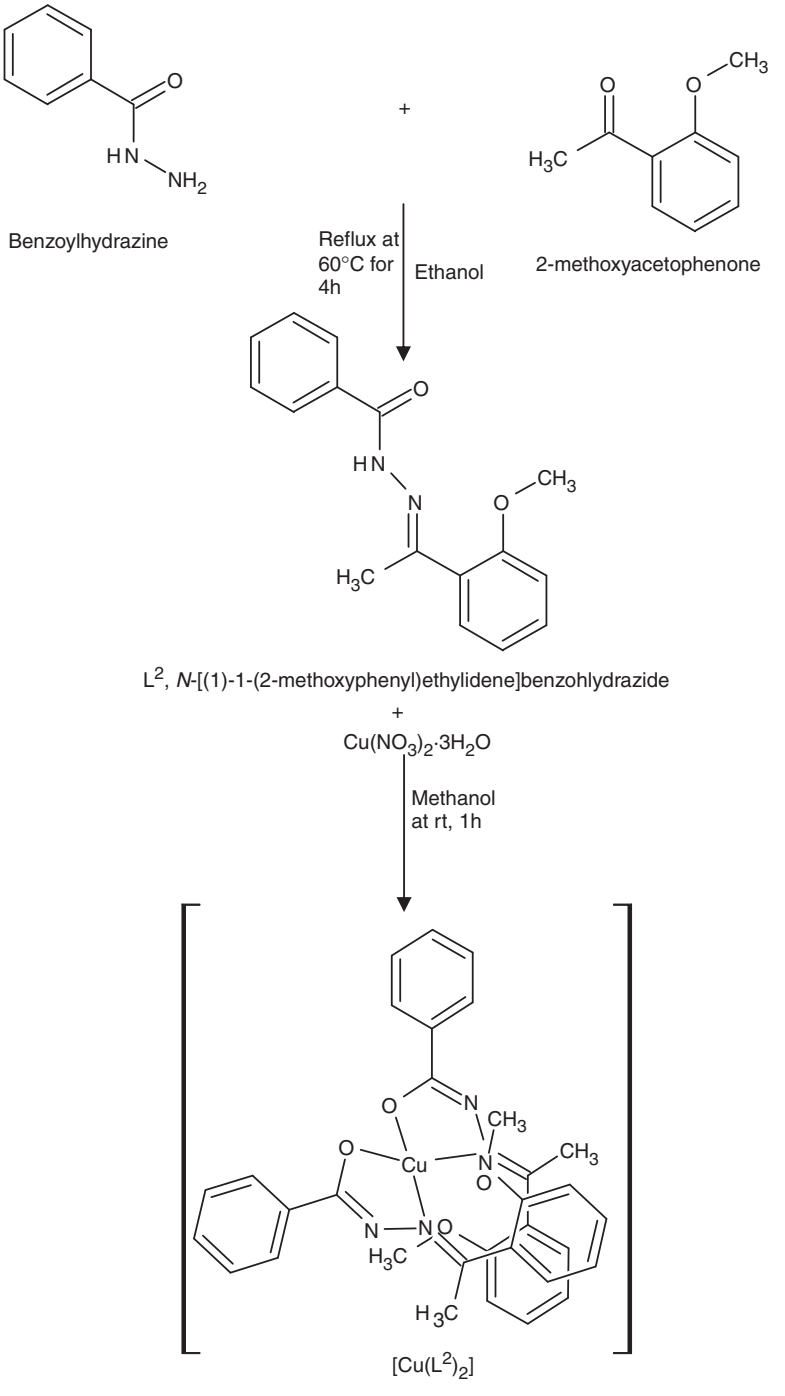

Scheme 2. Synthesis of L^2 and **4**.

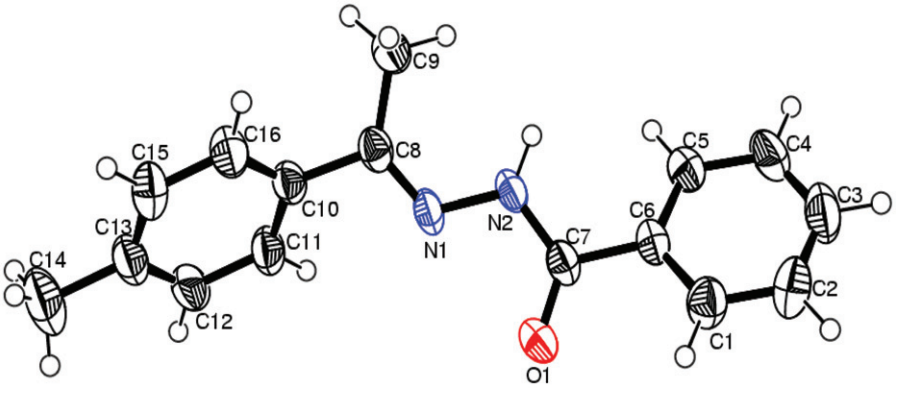

Figure 1. Projection view of (L^1) (**1**).

Table 1. Crystal data and structure refinement for **1**, **3**, and **4**.

Formula	$C_{16}H_{16}N_2O$	$C_{32}H_{30}CuN_4O_2$	$C_{32}H_{30}CuN_4O_4$
Formula weight	252.32	566.14	598.14
Space group	$P2_1/c$	$P2_1/c$	$P2/c$
Unit cell dimensions (Å, °)			
a	11.355(2)	9.524(19)	17.572(16)
b	14.140(3)	14.843(3)	9.378(6)
c	8.549(16)	20.398(4)	18.953(16)
α	90	90	90
β	102.59(2)	103.39(18)	115.26(11)
γ	90	90	90
Volume (Å^3), Z	1339.6(4), 4	2805.2(9), 4	2824.5(4), 4
Radiation	MoKα	MoKα	MoKα
Calculated density (Mg m^{-3})	1.251	1.340	1.407
Absorption coefficient (mm^{-1})	0.079	0.814	0.818
Reflections collected	9967	24464	22808
Unique	2359[R(int) = 0.0895]	4918[R(int) = 0.0456]	4971[R(int) = 0.0210]
θ range for data collection (°)	3.08 to 25.00	2.97 to 25.00	3.01 to 25.00
Max. and min. transmission	0.9898 and 0.9820	0.8945 and 0.8348	0.9011 and 0.8406
Final R indices	$R_1 = 0.0581$, $wR_2 = 0.1271$	$R_1 = 0.0457$, $wR_2 = 0.1364$	$R_1 = 0.0411$, $wR_2 = 0.1143$
R indices (all date)	$R_1 = 0.1191$, $wR_2 = 0.1539$	$R_1 = 0.0671$, $wR_2 = 0.1426$	$R_1 = 0.0504$, $wR_2 = 0.1169$

O1 ··· H(5)–C(5) = 3.153(.004). C–H ··· π non-covalent interaction (3.768 Å) may stabilize the structure (figure 2) [22]. (The distance 3.768 Å between Cg ··· H(14) represent C–H ··· π interaction where Cg is the centroid of phenyl ring.) Such an interaction stabilizes the structure in the solid state [23].

3.3. *Coordination chemistry of [Cu(L^1)$_2$] (3) and [Cu(L^2)$_2$] (4)*

Crystal structure refinement data related to **3** and **4** are given in table 1. The ORTEP views of **3** and **4** are shown in figures 3 and 4. The main bond angles and distances are

Table 2. Bond lengths (Å) and angles (°) for **1**.

O(1)–C(7)	1.226(3)	N(2)–C(7)	1.364(3)
N(1)–C(8)	1.279(3)	N(1)–N(2)	1.388(3)
C(8)–N(1)–N(2)	119.2(2)	N(2)–C(7)–C(6)	116.6(2)
C(7)–N(2)–N(1)	115.4(2)	N(1)–C(8)–C(10)	113.6(2)
C(2)–C(1)–C(6)	120.4(3)	N(1)–C(8)–C(9)	127.7(2)
C(8)–N(1)–N(2)	119.2(2)	O(1)–C(7)–N(2)	122.4(2)
C(7)–N(2)–N(1)	115.4(2)	O(1)–C(7)–C(6)	121.1(3)

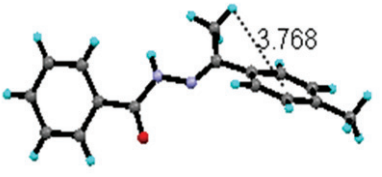

Figure 2. The C–H···π interaction in **1** involving the π···ring of the phenyl group and hydrogen of the methyl.

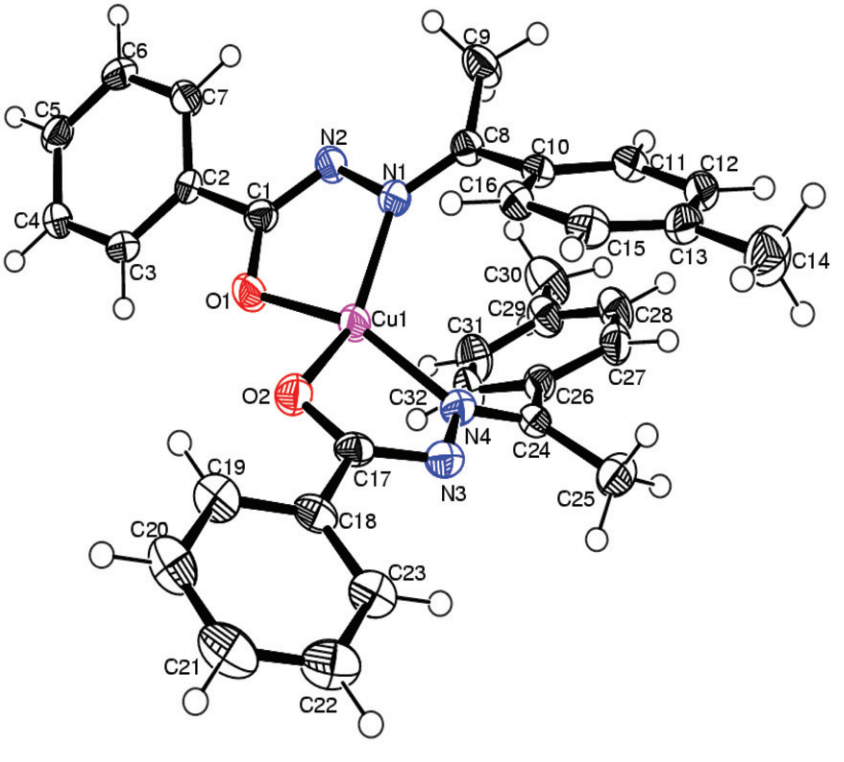

Figure 3. Projection view of $[Cu(L^1)_2]$ (**3**).

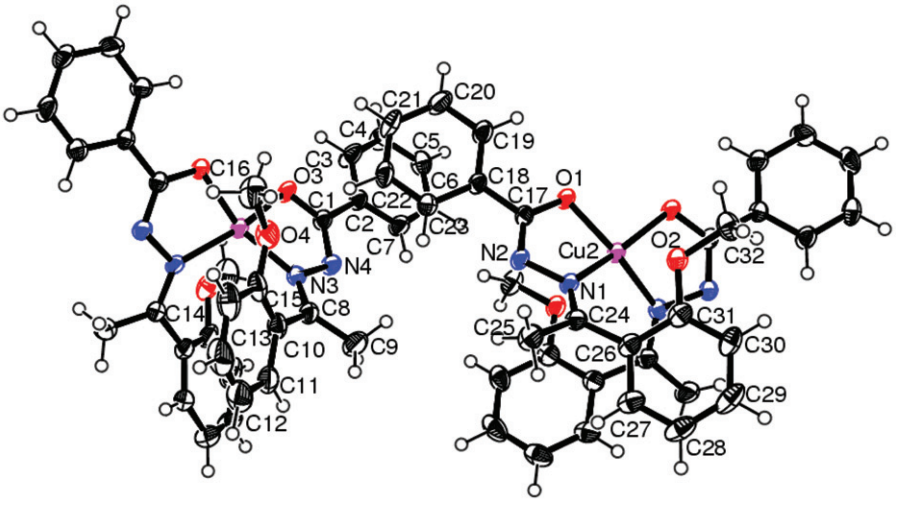

Figure 4. Projection view of $[Cu(L^2)_2]$ (**4**).

Table 3. Bond lengths (Å) and angles (°) for **3**.

Cu(1)–O(1)	1.900(2)	N(1)–C(8)	1.300(5)
Cu(1)–O(2)	1.908(2)	N(1)–N(2)	1.403(4)
Cu(1)–N(4)	1.966(3)	N(2)–C(1)	1.300(5)
Cu(1)–N(1)	1.987(3)	N(3)–C(17)	1.312(5)
O(1)–C(1)	1.290(4)	N(3)–N(4)	1.400(4)
O(2)–C(17)	1.287(4)	N(4)–C(24)	1.298(5)
O(1)–Cu(1)–O(2)	96.65(11)	C(1)–O(1)–Cu(1)	110.9(2)
O(1)–Cu(1)–N(4)	154.75(12)	C(17)–O(2)–Cu(1)	110.2(2)
O(2)–Cu(1)–N(4)	81.60(11)	C(8)–N(1)–Cu(1)	133.4(2)
O(1)–Cu(1)–N(1)	81.95(11)	N(2)–N(1)–Cu(1)	111.0(2)
O(2)–Cu(1)–N(1)	148.27(12)	C(24)–N(4)–Cu(1)	130.1(2)
N(4)–Cu(1)–N(1)	112.60(12)	N(3)–N(4)–Cu(1)	111.9(2)

presented in tables 3 and 4. Complex **3** crystallizes in the monoclinic crystal system, $P2_1/c$ space group, whereas **4** crystallizes with two monomers per asymmetric unit in the monoclinic crystal system. The molecules in the asymmetric unit are almost identical, so we limit discussion to one of the molecules. In both complexes Cu(II) is chelated by the ligand in 1:2 ratio and coordinated by two nitrogens and two oxygens. The five-membered chelate rings are co-coplanar. In both complexes two ligands are coordinated to Cu(II) equatorial. The Cu(1)–N(1) and Cu(1)–N(4) bond lengths 1.987(3) Å, 1.966(3) Å for **3** agree with those found for other copper Schiff-base complexes [12, 13]. In both complexes the Cu–O bond length is comparatively shorter than the sum of van der Waal's radii of oxygen and Cu (1.50 + 1.40 = 2.90 Å), indicating comparatively strong Cu–O bonding [24].

In **3** and **4** the C=N bond distances of 1.29 and 1.31 Å, close to the theoretical predicated value of C=N (1.28 Å) [20] confirm formation of Schiff base [21]. The bond distances of Schiff base donor and copper are 1.900(2)–1.987(3) Å for **3** and

Table 4. Bond lengths (Å) and angles (°) for **4**.

Cu(2)–O(1)#2	1.874(2)	Cu(2)–O(1)	1.874(2)
Cu(2)–N(1)#2	1.876(2)	Cu(2)–N(1)	1.876(2)
N(1)–C(24)	1.313(4)	N(1)–N(2)	1.383(3)
N(3)–C(8)	1.322(4)		
N(1)#2–Cu(2)–N(1)	103.48(15)	N(2)–N(1)–Cu(2)	106.57(18)
O(1)–Cu(2)–O(1)#2	92.86(12)	O(1)#2–Cu(2)–N(1)#2	85.99(9)
O(1)–Cu(2)–N(1)#2	157.44(10)	O(1)–Cu(2)–N(1)	85.99(9)
O(1)#2–Cu(2)–N(1)	157.44(10)		

Symmetry transformations used to generate equivalent atoms: #1 $-x+1$, y, $-z+3/2$; #2 $-x$, y, $-z+1/2$

1.874(2)–1.876(2) Å for **4**, close to ~1.9 Å typical of similar Cu(II) complexes [25]. All other bond lengths and angles on the ligand network are close to the expected value. The *cisoid* angles around copper in the square basal plane O(1)–Cu(1)–N(1) = 81.95(11), N(1)–Cu(1)–N(4) = 112.60(12), O(2)–Cu(1)–O(1) = 95.65(11) and N(4)–Cu(1)–O(2) = 81.60°(11) for **3** and N(1)–Cu(2)–O(1) = 85.99°(9), O(1)–Cu(2)–O(1)≠2 = 92.86°(12), O(1)≠2–Cu(2)–N(1)≠2 = 85.99°(9) and N(1)≠2–Cu(2)–N(1) = 103.48°(15) for **4** illustrate that **3** and **4** are slightly distorted from square planar geometry. The bite angles involving the Schiff base of **4** for the five-membered chelate rings are ~81.8° and ~86.0°. The geometry around Cu(II) is also evident from the value of *trans* angles N(1)–Cu(1)–O(2) = 148.27(12) and O(1)–Cu(1)–N(4) = 154.75(12) which deviate from the ideal value. Distortion of the square plane can also be determined by the dihedral angle between the CuNO planes. Thus, when the dihedral angle is 0° the geometry is planar, while when the angle is 90° the geometry is tetrahedral. The dihedral angles 42.53(0.014)° for **3** and 22.68(0.11)° for **4** reflect the degree of distortion from the plane. The rms deviations of the five-membered planes are 0.0662 and 0.0300 for **3** and 0.0972, 0.0035 and 0.087 for **4**. In **3** the distances of 1.644 Å and 1.649 Å between Cu(II) and the centroid defined by N(1)N(2)C(1)O(1) and N(4)N(3)C(17)O(3) planes and distance of 1.543 Å (for **4**) between Cu(II) and centroid defined by O(1)C(17)N(2)N(1) lead to ring metal interaction [26]. The significant distance of 3.284 Å (for **3**) and 3.081 Å (for **4**) between the two identical centroids leads to ring–ring interaction.

The geometry of **3** may stabilize the structure due to the C–H$\cdots\pi$ non-covalent interaction (3.222 Å) (figure 5) [22]. A similar C–H$\cdots\pi$ interaction is reported in a vanadium complex of the Schiff base [27]. The 3.222 Å between Cg$\cdots$H(25A) represent the C–H$\cdots\pi$ interaction where Cg is the centroid of the phenyl ring. Such an interaction stabilizes the structure in the solid state [24].

3.4. *Lattice structure and hydrogen bonding*

Complex **3** shows significant hydrogen bonding. Relevant hydrogen-bonding distances are given in table 5. The crystal packing is stabilized by a complicated H-bond network. Intramolecular hydrogen-bonding interaction (2.486(0.002) Å) is observed between O(1) of coordinated carbonyl and H(3) of the benzene ring. The oxygen of coordinated carbonyl and uncoordinated nitrogen of the hydrazone are also involved in intramolecular hydrogen bonding. The complex may stabilize the structure due to the presence of a C–H$\cdots\pi$ non-covalent interaction. The ketonic oxygen of carbonyl in **3** is intramolecularly hydrogen bonded to the methyl of **1**. As a consequence, there is an elongation of the Cu1–O1/Cu1–O2 length compared to **2**.

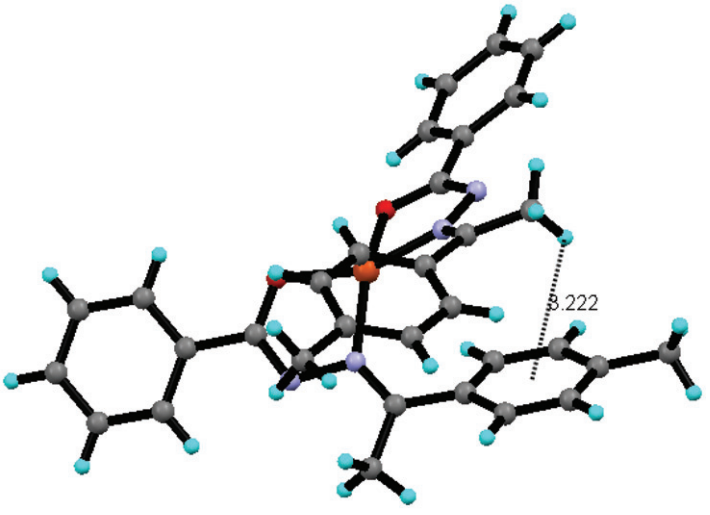

Figure 5. The C–H···π interaction in **3** involving the π···ring of the phenyl and hydrogen of the methyl.

Table 5. Intramolecular hydrogen bonds for **1** and **3** (Å and °).

Interactions	D–H (Å)	H···A (Å)	D···A (Å)	∠ D–H···A (°)	Symmetry operation
1					
C1–H1···O1 (0)	0.950 (0.003)	2.542 (0.002)	2.816 (0.003)	96.75(0.18)	x, y, z
C5–H5···N2 (0)	0.950 (0.003)	2.685 (0.002)	2.931 (0.003)	95.369(0.18)	x, y, z
C9–H9A···N2 (0)	0.980 (0.003)	2.572 (0.002)	2.869 (0.004)	97.46(0.19)	x, y, z
C11–H11···N1 (0)	0.950 (0.003)	2.612 (0.002)	2.809 (0.003)	91.91(0.17)	x, y, z
C2–H2···N2 (1)	0.950 (0.003)	2.792 (0.002)	3.742 (0.004)	179.12(0.21)	$-x+2, +y-1/2, -z+1/2$
C2–H2···N1 (1)	0.950 (0.003)	2.867 (0.002)	3.729 (0.004)	151.32(0.21)	$-x+2, +y-1/2, -z+1/2$
C5–H5···O1 (2)	0.950 (0.003)	2.380 (0.002)	3.153 (0.004)	138.29(0.19)	$x, -y+1/2, +z+1/2$
N2–H2N···O1 (2)	0.927 (0.031)	2.266 (0.030)	3.158 (0.003)	161.14(2.59)	$x, -y+1/2, +z+1/2$
C9–H9A···O1 (2)	0.980 (0.003)	2.353 (0.002)	3.320 (0.003)	168.86(0.18)	$x, -y+1/2, +z+1/2$
3					
C3–H3···O1 (0)	0.950 (0.004)	2.486 (0.002)	2.789 (0.004)	98.45(0.23)	x, y, z
C7–H7···N2 (0)	0.950 (0.004)	2.520 (0.003)	2.811 (0.004)	97.85(0.22)	x, y, z
C9–H9C···N2 (0)	0.980 (0.004)	2.551 (0.003)	2.685 (0.005)	87.04(0.25)	x, y, z
C16–H16···N1 (0)	0.950 (0.004)	2.728 (0.003)	2.934 (0.005)	92.90(0.23)	x, y, z
C19–H19···O2 (0)	0.950 (0.004)	2.440 (0.003)	2.750 (0.005)	98.76(0.25)	x, y, z
C23–H23···N3 (0)	0.950 (0.004)	2.539 (0.003)	2.839 (0.006)	98.45(0.25)	x, y, z
C25–H25C···N3 (0)	0.980 (0.004)	2.577 (0.003)	2.782 (0.005)	91.52(0.24)	x, y, z
C32–H32···N4 (1)	0.950 (0.004)	2.670 (0.003)	2.888 (0.005)	93.52(0.24)	$-x+1, -y, -z+1$
C30–H30B···O1 (3)	0.980 (0.005)	2.920 (0.003)	3.449 (0.006)	114.95(0.30)	$x-1, +y, +z$

The packing of the molecule in a unit cell is shown in figure 6. Viewed down the *c*-axis four molecules are arranged in the unit cell. It is evident from the figure that the unit cell as a whole is packed in a centrosymmetric manner.

3.5. *Electronic spectra*

Significant electronic absorption bands in spectra of **3** and **4** were recorded in DMSO at 25°C. For square planar complexes with $d_{x^2-y^2}$ ground state, three spin-allowed

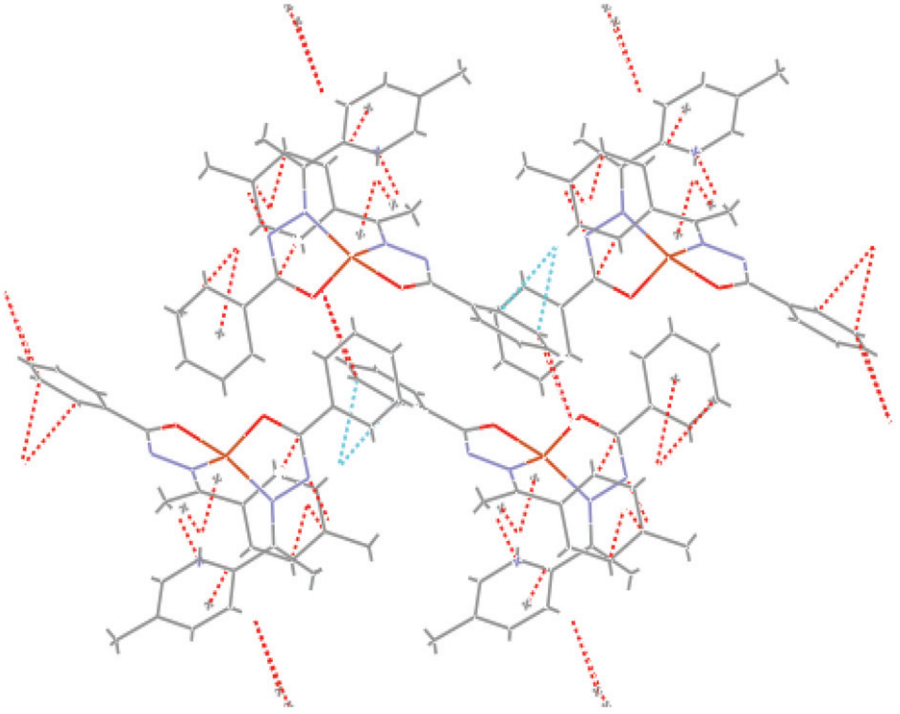

Figure 6. Unit cell packing of **4** at the c-axis.

transitions are possible, $^2B_{1g} \rightarrow {}^2A_{1g}$ ($d_{x^2-y^2} \rightarrow d_{z^2} \ldots \nu_1$), $^2B_{1g} \rightarrow {}^2B_{2g}$ ($d_{x^2-y^2} \rightarrow d_{xy}, \ldots, \nu_2$), and $^2B_{1g} \rightarrow {}^2E_g$ ($d_{x^2-y^2} \rightarrow d_{xz}, d_{yz}, \ldots, \nu_3$). Each spectrum exhibits a broad band centered at 700 and 650 nm, respectively, a characteristic of square planar geometry [28–30]. Due to the broadness of the band, other expected transitions in this range could not be assigned. The LMCT band for the complexes appeared at 585–400 nm with a shoulder at 350 nm.

3.6. *Molar conductivity*

Molar conductance values of **3** and **4** in 3×10^{-3} mol L^{-1} DMSO solution are 16 and 18 Ω^{-1} cm^2 mol^{-1}, indicating non-electrolytic behavior [31].

3.7. *Magnetic moment*

The magnetic susceptibilities of the solid complexes were determined at 298 K with a Gouy balance. Magnetic susceptibilities in the solid state show that the copper(II) complexes are paramagnetic at 298 K with magnetic moments close to the spin only ($S = +1/2$) 1.76 ± 0.3 BM, as expected from discrete and magnetically non-coupled mononuclear $3d^9$ ions. The magnetic moment values (μ_{eff}) of **3** and **4** are within the range described by earlier workers [32].

Table 6. EPR spectral parameters of the copper(II) complexes.

EPR parameter	3	4
Polycrystalline state (298 K)		
$g_{\parallel}$	2.2598	2.2411
$g_{\perp}$	2.0661	2.0152
DMSO (77 K)		
$g_{\parallel}$	2.2153	2.2406
$g_{\perp}$	2.0406	2.0535
$A_{\parallel}$ (G)	180	175
G	5.56	4.08
α^2	0.793	0.752
β^2	0.855	0.926
γ^2	0.726	0.917
$K_{\perp}$	0.574	0.689
$K_{\parallel}$	0.677	0.743
f (cm)	131	135

3.8. *Infrared spectral study*

In IR spectra of **3** and **4** the band at 1640 cm^{-1}, which is attributed to ν(C=N), confirms the formation of Schiff base [33]. This band is shifted to lower frequencies by ca-15–20 cm^{-1}, indicating coordination *via* the azomethine nitrogen. This is confirmed by bands at 459–461 cm^{-1}, assigned to ν(Cu–N) [34]. The presence of a strong sharp band at 1257 cm^{-1} can be attributed to ν(C–O). New bands with medium to weak intensities at 395–505 cm^{-1} are tentatively assigned to ν(M–O)/(M–N) [34].

Based on the above spectral evidences, it is confirmed that the ligand is coordinated bidentate to the metal *via* the azomethine nitrogen and carbonyl oxygen. Thus the IR spectral data provide evidence for complexation of the bidentate ligands.

3.9. *Electron paramagnetic resonance spectra*

3.9.1. Solid state spectra. EPR spectra of powder samples were obtained at 300 K with EPR parameters of **3** and **4** listed in table 6. Polycrystalline EPR spectra of **3** and **4** are typical of monomeric distorted tetragonal copper(II) complexes with $d_{x^2-y^2}$ ground state ($g_{\parallel} > g_{\perp} > g_e$) [35], exhibit only one exchange-averaged broad signal which is attributable to nonequivalent Cu(II) centers in the solid [36]. EPR spectra of powder sample of **3** display four copper hyperfine lines in the parallel region, indicating that **3** is monomeric. According to Hathaway [37] if $G > 4$ exchange interaction is negligible and $G < 4$ indicates exchange interaction. The value of G of 5.5 for **3** and 4.1 for **4** indicate exchange interaction is negligible in solid state.

3.9.2. Solution EPR spectra. EPR spectra of the complexes in DMSO at 77 K are given in figure 7 and Supplementary material, figure S1. Four hyperfine lines are observed which arise from coupling of the odd electron with copper nucleus (^{65}Cu, $I = \pm 3/2$). The spectra of these complexes at 77 K are typical axial with well-resolved hyperfine lines showing nitrogen superhyperfine lines in the $g_{\perp}$ region.

EPR parameters and d–d transition energies were used to evaluate α^2, β^2, and γ^2, which may be regarded as measures of the covalency of the in-plane σ bonding, in-plane

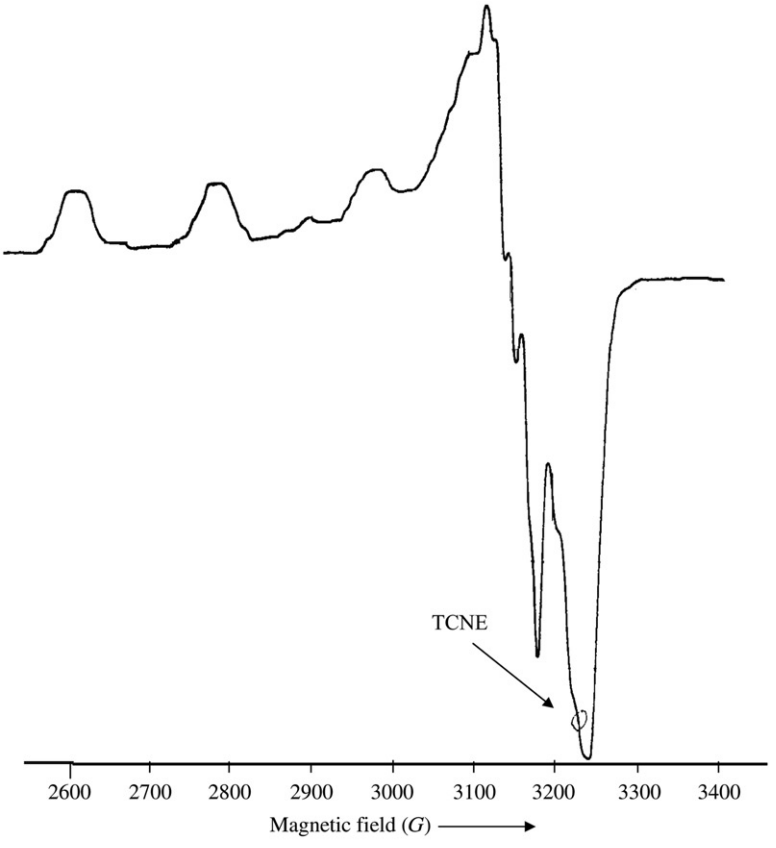

Figure 7. EPR spectra of **3** in DMSO (0.003 $mol^{-1}\,dm^{-3}$) at 77 K.

π- and out-of-plane π-bonding, respectively. The in-plane σ-bonding parameter α^2 was calculated from [38]:

$$\alpha^2 = (A_{||}/0.036) + (g_{||} - 2.0023) + 3/7(g_{\perp} - 2.0023) + 0.04.$$

The orbital reduction factors $K_{\parallel}$ and $K_{\perp}$ were estimated from the expressions [39]:

$$K_{\parallel}^2 = (g_{||} - 2.0023)\ E_{d-d}/8\lambda_0,$$
$$K_{\perp}^2 = (g_{\perp} - 2.0023)E_{d-d}/2\lambda_0,$$

where $K_{\parallel} = \alpha^2\ \beta^2$, $K_{\perp} = \alpha^2\ \gamma^2$, and λ_0 represents the one electron spin–orbit coupling constant for the free ion, equal to $-828\,cm^{-1}$. Significant information about the nature of bonding in the copper(II) complexes can be derived from the magnitude of $K_{\parallel}$ and $K_{\perp}$. For pure σ bonding $K_{\parallel} \approx K_{\perp} \approx 0.77$ whereas $K_{\parallel} < K_{\perp}$ implies considerable in-plane bonding, while for out-of-plane bonding, $K_{\parallel} > K_{\perp}$. In the present copper(II) complexes $K_{\parallel} > K_{\perp}$, indicating significant out-of-plane bonding. The values of α^2, β^2, and γ^2 of the complexes are consistent with both strong in-plane σ and in-plane π bonding. The empirical factor $f = g_{||}/A_{||}$ ($A_{||}$ in cm^{-1}) is an index of tetragonal distortions varying from 105 to 135 cm for small to extreme distortions in square planar complexes [40]. The f values of 131 cm for **3** and 135 cm for **4** indicate distortion from planarity.

Table 7. Cyclic voltammetric data for 1 m mol L^{-1} solution of the Cu(II) complexes in DMSO containing 0.1 mol L^{-1} $NaClO_4$ as supporting electrolyte.

Scan rate ($mV\,s^{-1}$)	E_{pc} (mV)	I_{pc} (μA)	E_{pa} (mV)	I_{pa} (μA)	ΔE_p (mV)	$E^{0'}$ (mV)	I_{pa}/I_{pc} (μA)
1							
100	178	0.989	436	1.130	257	307	1.143
200	169	1.2833	450	1.466	281	309	1.138
300	160	2.143	458	2.466	298	309	1.151
3							
100	106	1.12	426	0.897	320	266	0.801
200	116	1.404	428	1.101	312	272	0.784
300	123	2.948	430	2.456	307	377	0.833
4							
100	−75	1.402	157	1.211	233	41.0	0.864
200	−91	1.563	174	1.322	265	42.0	0.846
300	−115	2.301	198	1.996	313	42.0	0.867

$\Delta E_p = E_{pa} - E_{pc}$; $E^{0'} = (E_{pa} + E_{pc})/2$.

Table 8. IC_{50} values and kinetic constant of **3** and **4**.

Complex	IC_{50} (μmol)	k_{McCF} ($mol\,L^{-1}\,s^{-1}$)[b] × 10^4
$[Cu(L^1)_2]$	49	1.939
$[Cu(L^2)_2]$	70	1.356

k_{McCF} were calculated by $K = k_{NBT} \times [NBT]/IC_{50}$, k_{NBT} (pH 7.8) = 5.94×10^4 mol $L^{-1}\,s^{-1}$ [43].

3.10. *Cyclic voltammetry*

The electrochemical behaviors have been studied by cyclic voltammetry using a glassy carbon electrode in DMSO under an inert atmosphere. A representative cyclic voltammogram is shown in "Supplementary material", figure S2, and the results are presented in table 7. The redox behavior of both complexes is similar, showing two redox processes in DMSO. The voltammetric behaviors are characterized by two fairly broad peaks as the cathodic and anodic waves. Peak potentials (table 7) are shifted going to faster scan rate. Both complexes exhibit one electron quasi-reversible cyclic voltammetry response. The separation between potential peaks ($\Delta E_p = E_{pa} - E_{pc}$) varies from 233 to 313 mV for **4**, characteristic of quasi-reversible process [41]. The low intensity redox peaks at high negative potential are assigned to reduction and oxidation of ligand. The reduced species is unstable in the voltammetric time scale as evidenced from the less than unity value of the I_{pa}/I_{pc} ratio, indicative of electron transfer reaction followed by a chemical reaction (EC mechanism) [42].

3.11. *SOD activity*

SOD reduces NBT chloride monohydrate. The metal complexes compete with NBT for oxidation of the generated superoxide ions in SOD-like activity experiments. The IC_{50} data of the SOD activity assay along with kinetic catalytic constants of **3** and **4** [43] are presented in table 8. The IC_{50} values are 49 and 70 μmol for **3** and **4**, respectively.

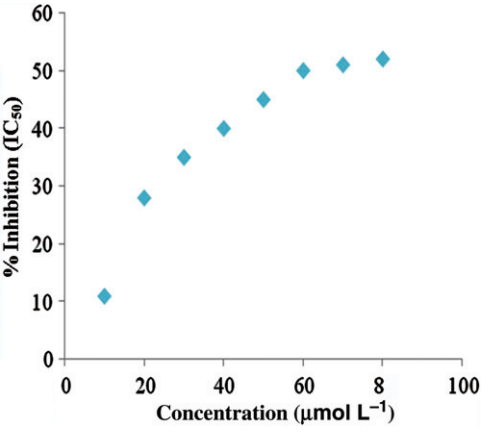

Figure 8. SOD activity of **3**.

The observed IC_{50} values (figure 8) of the present complexes are comparable to reported values for copper(II) complexes, but are less active than the native SOD. Both complexes have similar SOD-like activity that corresponds to reported mononuclear copper complexes which have high SOD-like activity [12, 13, 44–47]. Weaker SOD-like activity may be attributed to greater steric hindrance of the coordinating molecule, hindering the action of O_2^-. The difference in IC_{50} values for the two complexes is ascribed to the discrepancy between their structures.

3.12. *Antibacterial activity*

Present complexes were evaluated against *E. coli* bacteria as the test organism as a function of concentration. The susceptibility of the present copper(II) complexes were determined by measuring the size of inhibition diameter. The growth inhibitory effects were observed against *E. coli*, which causes dysentery and food poisoning, respectively. Both complexes are effective against *E. coli* with zone of inhibition less for 1 mmol L^{-1} and more in 3 mmol L^{-1}. For **3** inhibition zone (18 mm) is larger (Supplementary material, figure S3) than **4**. Similar antimicrobial results were reported by Tarafder *et al.* [48] and also by our school [49–51] on simple copper(II) binary and ternary complexes.

4. Conclusion

This article clearly demonstrates new ligands and their complexes, $[Cu(L)_2]$. The backbone of the ligands accommodates copper(II) because of their flexibility and constraints imposed by the ligands themselves. Voltammetric studies gave evidence to a quasi-reversible process that could be attributed to a dynamic rearrangement of the coordination environment during the redox process. The presence of H-bonding and C–H $\cdots \pi$ interaction also stabilize the molecule in a solid state. In both complexes copper center is four-coordinate with distortion from square planar geometry.

Supplementary material

CCDC nos 766591, 766592, and 766593 contain the supplementary crystallographic data for L^1, $[M(L^1)_2]$, and $[M(L^2)_2]$, where $L^1 = 1$-phenyl-2-ene-2-(4-methylphenyl)-prop-1-one and $L^2 = 1$-phenyl-2-ene-2-(2-methylphenyl)-prop-1-one. These data can be obtained free of charge *via* http://www.ccdc.cam.ac.uk/conts/retrieving.html, or from the Cambridge Crystallographic Data Centre, 12 Union Road, Cambridge CB2 1EZ, UK; Fax (+44) 1223-336-033; or E-mail: deposit@ccdc.cam.ac.uk.

Acknowledgments

Our sincere thanks are due to the National Diffraction Facility, X-ray Division, and RSIC (SAIF), IIT Mumbai for single crystal data collection and EPR measurements, respectively. The Head RSIC (SAIF), Central Drug Research Institute, Lucknow is also thankfully acknowledged for providing analytical and spectral facilities. Financial assistance from UGC [Scheme no. 36-28/2008 (SR)] and DRDO [Scheme no. ERIP/Er/0603574/M/01/1118] Delhi are also thankfully acknowledged.

References

[1] C. Muscoli, S. Cuzzocrea, D.P. Riley, J.L. Zweier, C. Thiemermann, Z.Q. Wang, D. Salvemini. *Br. J. Pharmacol.*, **140**, 445 (2003).
[2] L.W. Oberlay. *Biomed. Pharmacother.*, **59**, 143 (2005).
[3] D. Salvemini, D.P. Riley, S. Cuzzocrea. *Nat. Rev. Drug Discovery*, **1**, 367 (2002).
[4] R. Pogni, M.C. Baratto, E. Busi, R. Basosi. *J. Inorg. Biochem.*, **73**, 157 (1999).
[5] D. Bose, J. Banerjee, S.H. Rahaman, G. Mostafa, H.-K. Fun, R.D. Bailey Walsh, M.J. Zaworotko, B.K. Ghosh. *Polyhedron*, **23**, 2045 (2004).
[6] M.J. Zaworotko. *Chem. Commun.*, 199 (2002).
[7] L. Rong-Guang, T. Zhu, X. Sai-Feng, Z. Qian-Jiang, W.G. Jackson, W. Zhan-Bing, L. La-Sheng. *Polyhedron*, **22**, 3467 (2003).
[8] C.P. Horwitz, S.E. Creager, R.W. Murray. *Inorg. Chem.*, **29**, 1006 (1990).
[9] A.S. Al-Shihri. *Spectrochim. Acta, Part A*, **60**, 1189 (2004).
[10] M. Yuan, F. Zhao, W. Zhang, Z.M. Wang, S. Gao. *Inorg. Chem.*, **46**, 11235 (2007).
[11] B.R. Manzano, F.A. Jalón, I.M. Ortiz, M.L. Soriano, F.G. de la Torre, J. Elguero, M.A. Maestro, K. Mereiter, T.D.W. Claridge. *Inorg. Chem.*, **47**, 413 (2008).
[12] R.N. Patel. *J. Coord. Chem.*, **63**, 1207 (2010).
[13] R.N. Patel, K.K. Shukla, A. Singh, M. Choudhary, D.K. Patel. *J. Coord. Chem.*, **63**, 586 (2010).
[14] G. Glugliarelli, S. Cannistraro. *Nuovolimento*, **4D**, 194 (1984).
[15] R.G. Bhirud, T.S. Srivastava. *Inorg. Chim. Acta*, **179**, 125 (1991).
[16] D. Liu, K. Kwasniewska. *Bull. Environ. Contam. Toxicol.*, **27**, 289 (1981).
[17] G.M. Sheldrick, SHELXS, *Program for the Solution for Crystal Structures*, University of Göttingen, Göttingen, Germany (1997).
[18] G.M. Sheldrick, SHELXL-97. *Program for the Refinement of Crystal Structures*, University of Göttingen, Germany (1997).
[19] C.K. Johnson, ORTEP, III Report ORNL- 5138, Oak Ridge National Laboratory, Oak Ridge, TN (1976).
[20] J. March. *Advanced Organic Chemistry, Reactions Mechanisms and Structure*, 4th Edn, Wiley, New York (1992).
[21] A.T. Chaviara, P.J. Cox, K.H. Repana, A.A. Pantazaki, K.T. Papazisis, A.H. Kortsaris, D.A. Kyriakidis, G.S. Nikolov, C.A. Bolos. *J. Inorg. Biochem.*, **99**, 467 (2005).
[22] H. Brunner. *Angew. Chem, Int. Ed. Engl.*, **22**, 897 (1983).
[23] P.S. Subramanian, E. Suresh, P. Dastidar, S. Waghmode, D. Srinivas. *Inorg. Chem.*, **40**, 4291 (2001).

[24] M. Singh, V. Agarwal, U.P. Singh, N.K. Singh. *Polyhedron*, **28**, 195 (2009).
[25] A.G. Raso, J.J. Friol, B. Adrover, P. Tauler, A. Pons, I. Mata, E. Espinosa, E. Molins. *Polyhedron*, **22**, 3255 (2003).
[26] M. Joseph, M. Kuriakose, M.R.P. Kurup, E. Suresh, A. Kishore, S.G. Bhat. *Polyhedron*, **25**, 61 (2006).
[27] S. Mondal, S.P. Rath, S. Dutta, A. Chakravorty. *J. Chem. Soc., Dalton Trans*., 1115 (1995).
[28] W.G. Hanna, M.M. Moaward. *Transition Met. Chem*., **26**, 644 (2001).
[29] K.E.M. Said. *Indian J. Chem*., **33A**, 830 (1994).
[30] A.B.P. Lever. *Inorganic Electronic Spectroscopy*, Elsevier, Amsterdam (1968).
[31] W.J. Geary. *Coord. Chem. Rev*., **78**, 81 (1971).
[32] M.F. El-Shazly, A. El-Dissowky, J. Salem, M. Osman. *Inorg. Chim. Acta*, **40**, 1 (1980).
[33] A.T. Chaviara, P.C. Christidis, A. Papageorgiou, E. Chrysogelou, D.J. Hadjipavlou-Litina, C.A. Bolos. *J. Inorg. Biochem*., **99**, 2102 (2005).
[34] K. Nakamoto. *Infrared and Raman Spectra of Inorganic and Coordination Compounds*, 5th Edn, Wiley, New York (1997).
[35] F.F. Boas, R.H. Dunhill, J.R. Pilbrow, R.C. Srivastava, T.D. Smith. *J. Chem. Soc. A*, 94 (1969).
[36] B.J. Hathaway, A.A.G. Tomlinson. *Coord. Chem. Rev*., **5**, 1 (1970).
[37] R.J. Rudley, B.J. Hathaway. *J. Chem. Soc*., 1725 (1970).
[38] G.F. Bryce. *J. Phys Chem*., **70**, 3549 (1966).
[39] D.X. West. *J. Inorg. Nucl. Chem*., **43**, 3169 (1984).
[40] R. Pogni, M.C. Bartoo, A. Diaz, R. Basosi. *J. Inorg. Biochem*., **79**, 333 (2000).
[41] G. Tabbi, W.L. Driessen, J. Reedijk, R.P. Bonomo, N. Veldman, A.L. Spek. *Inorg. Chem*., **36**, 1168 (1997).
[42] S. Perveen, F. Arjmond. *Indian J. Chem*., **44A**, 1151 (2005).
[43] Z.-R. Liao, X.-F. Zheng, B.-S. Luo, L.-R. Shen, D.-F. Li, H.-L. Liu, W. Zhao. *Polyhedron*, **20**, 2813 (2001).
[44] Y.H. Zhou, H. Fu, W.X. Zhao, W.L. Chen, C.Y. Su, H. Sun, L.N. Ji, Z.W. Mao. *Inorg. Chem*., **46**, 734 (2007).
[45] M. González-Álvarez, G. Alzuet, J. Borras, L.C. Agudo, S. García-Granda, J.M. Montejo-Bernardo. *Inorg. Chem*., **44**, 9424 (2005).
[46] L.L. Costanjo, G. Degudi, S. Giuffrida, E. Rizzarelli, G. Vecchio. *J. Inorg. Biochem*., **50**, 273 (1993).
[47] R.G. Bhirud, T.S. Srivastava. *Inorg. Chim. Acta*, **178**, 121 (1990).
[48] M.T.H. Tarafder, K.B. Chew, K.A. Crouse, A.M. Ali, B.M. Yamin, H.K. Fun. *Polyhedron*, **21**, 2683 (2002).
[49] N. Singh, K.K. Shukla, R.N. Patel, U.K. Chauhan, R. Shrivastava. *Spectrochim. Acta, Part A*, **59**, 3111 (2003).
[50] R.N. Patel, N. Singh, K.K. Shukla, U.K. Chouhan, J. Niclos-Gutierrez, A. Castineiras. *Inorg. Chim. Acta*, **357**, 2469 (2004).
[51] R.N. Patel, A. Singh, K.K. Shukla, D.K. Patel, V.P. Sondhiya, S. Dwivedi. *J. Sulf. Chem*., **31**, 299 (2010).